Laser heating of an aqueous aerosol particle

Gideon Sageev and John H. Seinfeld

Approximate analytical and full numerical solutions are obtained for the transient response of both a pure water and solution droplets to both short- and long-time laser heating. The differences in the temperature and size histories between pure water and solution droplets are elucidated. The validity of of the approximate analytical solution, extended from that of Armstrong ["Aerosol Heating and Vaporization by Pulsed Light Beams," Appl. Opt. **23**, 148 (1984)] in pure water droplets, is evaluated by comparison to solution of the full governing equations.

I. Introduction

Heating an aerosol particle on irradiation with a laser beam induces temperature gradients in the air surrounding the particle that change the air's index of refraction in the vicinity of the particle. These changes may cause the beam to diverge as it passes through the medium. To estimate the magnitude of this phenomenon, called thermal blooming, the particle's surface temperature must be known.

The amount of energy a particle absorbs from the incident light beam depends on the particle's complex index of refraction as well as on its optical size (where the optical size x is given by $x = 2\pi r_s/\lambda$, r_s and λ being the particle radius and laser wavelength, respectively). In this work, the beam wavelengths considered are much larger than the particle radius; thus the energy absorbed by the particle can be obtained from Rayleigh theory.[1] As the optical size of the particle increases, the absorption of energy by the particle may be enhanced by structure resonance;[2] however, in the present work, this effect is neglected.

The particles considered here are homogeneous liquid drops containing a solute. When the incident beam first strikes a volatile particle (which is assumed to be initially in equilibrium with its environment), all the absorbed energy goes into raising the particle's temperature. As the particle's temperature increases, the solvent in the particle begins to vaporize, and, at the same time, energy is lost from the particle by conduction into the gas phase. The processes of mass and heat transfer in the air surrounding the drop can be assumed to be at a pseudo-steady state as long as the characteristic times for changes in the temperature and concentration profiles in the gas are much shorter than that for the temperature of the drop. This is generally a good assumption for the drops of interest here. The relative amounts of energy dissipated by conduction and evaporation depend strongly on the presence of solutes in the drop. The effect of the solutes is to lower the vapor pressure of the solvent in the drop, thereby lowering the vaporization rate from that in the absence of solutes. As the vaporization continues, the solution droplet shrinks and approaches a new steady state size and temperature, at which point all the absorbed heat is released by conduction.

In a pure droplet, on the other hand, the evaporation rate is governed only by the effect of the droplet temperature on its vapor pressure. Since solutes are absent, the vaporization from the drop continues until the drop disappears. Thus, in a pure droplet, a fraction of the absorbed energy is always dissipated by vaporization.

The above description refers to situations in which either a solvent/solute droplet or a pure solvent droplet is continually heated with a laser. An alternative situation of practical interest is that in which a pulsed laser is used and the particle is heated by the laser for only a short period of time. When a pure solvent droplet is subject to a short pulse of laser light, its temperature increases initially before significant evaporation or conduction into the gas phase can take place. Consequently, in a short heating period, the particle can be assumed not to shrink due to loss of material by evaporation. When the laser is turned off, the droplet is no longer in equilibrium with its surroundings, and it begins to cool by the combined effects of conduction and vaporization. Eventually, the drop reaches a new equilibrium size at which point its temperature returns to that of its surroundings. The total amount of mass lost is related to the total energy input into the drop. When a solution drop is subject to a short-period laser

The authors are with California Institute of Technology, Department of Chemical Engineering, Pasadena, California 91125.

Received 27 June 1984.
0003-6935/84/234368-07$02.00/0.

heating, its temperature also rises quickly before appreciable conduction or evaporation can take place. After the laser is turned off, the droplet returns to its original temperature. However, eventually the droplet also returns to its initial equilibrium size due to replenishment of solvent from the vapor.

The aerosol temperature rise resulting from the long-time heating of a pure water drop by a laser beam was investigated numerically by Caledonia and Teare.[3] More recently, Armstrong[4] obtained an analytical solution to the heating of a pure water droplet by making a number of assumptions. First, Armstrong assumed that once the laser is turned on, even though conduction and vaporization are occurring during the heating process, the radius of the drop remains at its initial value. Eventually, a steady state is reached where the absorbed laser energy is balanced by energy losses due to conduction and vaporization, still assuming the particle retains its initial size. Once at steady state, the particle temperature is assumed to stay constant throughout the remaining heating period. The change in radius of the drop is then approximated from the solvent mass flux based on the steady state temperature of the drop. The assumption of constant particle size during the short heating times enables an analytical solution to be obtained.

Both works cited above apply to the heating of a pure water droplet. However, since atmospheric aerosols must contain solutes to exist in equilibrium in an environment where the relative humidity is <100%, it is important to investigate the effect of the presence of solutes on the aerosol heating process.

The main object of the present work is to obtain both approximate analytical and full numerical solutions to the transient response of both pure solvent and solution droplets to both short- and long-time laser heating. We will examine the differences between the temperature rise in a solution and that in a pure droplet. Also, by calculating the temperature rise by solving the full governing equations numerically, we can evaluate the validity of the approximate analytical solution.

In Sec. II, we develop the theory of heat and mass transfer from a droplet subject to internal heating. Section III is devoted to the thermodynamic data used in calculation of the droplet temperature rise. In Sec. IV, the analytical and numerical results based on a short heating period are shown and discussed. Finally, in Sec. V we present numerical results based on a long heating period.

II. Theory

The equations governing the concentration and temperature profiles surrounding a volatile particle that contains an internal heating source are well known.[5] In such a situation, when the Biot number in the drop–air system is much smaller than unity, the drop temperature can be assumed to be constant. In doing so, the overall energy balance over the drop is given by

$$\rho_d C_d \frac{dT}{dt} = I_0\alpha - \frac{3}{r_s}\left[-LD_a\left(\frac{\partial Y}{\partial r}\right)_{r=r_a} - k_a\left(\frac{\partial T}{\partial r}\right)_{r=r_a}\right], \quad (1)$$

where T and t are temperature and time; Y and D_a are the water mass fraction and diffusivity in the air; I_0 and α are the incident beam intensity and bulk absorption coefficient; C_d, k_a, and L are the heat capacity, thermal conductivity, and heat of vaporization; and ρ_d and r_s are the drop density and radius. The subscripts s, a, and d refer to conditions of the surface, air, and drop, respectively.

On the right-hand side of Eq. (1), $I_0\alpha$ is the heat source. The first term inside the brackets is due to mass transfer across the interface, while the second term is due to heat conduction from the surface. Both of the gradients $(\partial Y/\partial r)_{r=r_s}$ and $(\partial T/\partial r)_{r=r_s}$ appearing in Eq. (1) depend on the boundary conditions at the drop surface and far away from the drop. When the unsteady terms are neglected in the equations of mass and heat transfer outside the drop, the mass and heat fluxes from the drop surface are given by[6]

$$-D_a\left(\frac{\partial Y}{\partial r}\right)_{r=r_s} = J = \frac{D_a}{r_s}\ln\left(\frac{1-Y_\infty}{1-Y_s}\right), \quad (2)$$

$$-k_a\left(\frac{\partial T}{\partial r}\right)_{r=r_s} = \frac{JC_a(T_s - T_\infty)}{L\left[\exp\left(\frac{r_s JC_a}{k_a}\right) - 1\right]}, \quad (3)$$

where J is the mass flux, Y_∞ and T_∞ are the water mass fraction and temperature far away from the drop, and Y_s and T_s are the analogous properties at the surface.

When Eqs. (2) and (3) are substituted into Eq. (1) one obtains[4]

$$\frac{dT}{dt} = \frac{I_0\alpha}{\rho_d C_d} - \frac{3JL}{r_s\rho_d C_d}\left\{1 + \frac{C_a(T - T_\infty)}{L\left[\exp\left(\frac{r_s JC_a}{k_a}\right) - 1\right]}\right\}. \quad (4)$$

For a solution droplet,

$$Y_s(T) \approx a_w(T)Y^0(T), \quad (5)$$

where a_w is the water activity and Y^0 is the water mass fraction resulting from the vapor pressure of pure water at temperature T. Assuming that the vapor at the surface is at equilibrium with the drop, $Y^0(T)$ can be related to $Y^0(T_\infty)$ by using the Clausius-Clapeyron and the Kelvin equations. The resulting expression is

$$Y^0(T) = Y^0(T_\infty)\exp\left[-\frac{LM_w}{R}\left(\frac{1}{T} - \frac{1}{T_\infty}\right)\right]\exp\left(\frac{2\bar{v}\sigma}{RTr_s}\right), \quad (6)$$

where M_w is the water molecular weight and R, $\bar{v}$, and σ are the gas constant, the solution molar volume, and the surface tension, respectively.

The water activity can be expressed in terms of the solute molality m, the total number of ions the solute molecule dissociates into ν, and the molal osmotic coefficient φ (Refs. 7 and 8):

$$a_w(T) = \exp\left[-\frac{\nu m M_w}{1000}\varphi(T)\right]. \quad (7)$$

The osmotic coefficients is related to the solute activity coefficient γ by

$$\varphi(T) = 1 + \frac{1}{m}\int_0^m m\,d\ln[\gamma(T)]. \quad (8)$$

Finally, the temperature dependence of γ is obtained from the Van't Hoff equation:[7]

$$\frac{\partial}{\partial T}(\ln\gamma^2)_P = \frac{\overline{H}_i^0 - \overline{H}_i}{RT^2}, \tag{9}$$

where $\overline{H}_i^0$ and $\overline{H}_i$ are the partial molal enthalpies of the solute at infinite dilution and molality m, respectively. By integration of Eq. (9) with respect to T, followed by differentiation with respect to m and substitution into Eq. (8), we obtain the following equation for the temperature dependence of the osmotic coefficient:

$$\varphi(T) = \varphi(T_\infty) + \left(\frac{1}{T} - \frac{1}{T_\infty}\right)\frac{1}{m}\int_0^m m'\frac{\partial}{\partial m'}\left[\frac{(\overline{H}_i - \overline{H}_i^0)}{2R}\right]dm' - \left(\ln\frac{T}{T_\infty} + \frac{T_\infty}{T} - 1\right)\frac{1}{m}\int_0^m m'\frac{\partial}{\partial m'}\left[\frac{(\overline{C}_i - \overline{C}_i^0)}{2R}\right]dm', \tag{10}$$

where $\overline{C}_i$ and $\overline{C}_i^0$ are the the partial molal heat capacities of the solute at molality m and at infinite dilution, respectively. In Eq. (10), we assume that the partial molal heat capacities remain constant with temperature. The solution of Eq. (10) requires osmotic coefficient data as well as thermodynamic data concerning the partial molal enthalpy and heat capacity. Data on $\varphi(T_\infty)$ at $T_\infty = 25°C$ for many salts can be found in a comprehensive report by Hamer and Wu.[9] By expressing the partial molal quantities in power series,[7] the integrals in Eq. (10) reduces to the following series:

$$\delta = \frac{1}{m}\int_0^m m'\frac{\partial}{\partial m'}\left[\frac{(\overline{H}_i - \overline{H}_i^0)}{2R}\right]dm' = \sum_{n=1} A_n\left(\frac{n}{n+2}\right)m^{n/2}, \tag{11}$$

$$\beta = \frac{1}{m}\int_0^m m'\frac{\partial}{\partial m'}\left[\frac{(\overline{C}_i - \overline{C}_i^0)}{2R}\right]dm' = \sum_{n=1} B_n\left(\frac{n}{n+2}\right)m^{n/2}, \tag{12}$$

where A_n and B_n are fitting parameters to experimental data. Once Eq. (10) is solved, the water activity is found by substitution into Eq. (7). Equation (2) can now be rewritten as

$$J = \frac{D_a}{r_s}\ln\left[\frac{1 - Y_\infty}{f(T)}\right], \tag{13}$$

where $f(T)$ is given by

$$f(T) = 1 - Y^0(T_\infty)\exp\left\{\frac{A}{T} - B\left[\varphi T_\infty) + \delta\left(\frac{1}{T} - \frac{1}{T_\infty}\right) - \beta\left(\ln\frac{T}{T_\infty} + \frac{T_\infty}{T} - 1\right)\right] - C\left(\frac{1}{T} - \frac{1}{T_\infty}\right)\right\}, \tag{14}$$

and where

$$A = \frac{2\bar{v}\sigma}{Rr_s}, \quad B = \frac{\nu m M_w}{1000}, \quad C = \frac{LM_w}{R}.$$

Since a numerical solution to Eq. (4) can be obtained readily, an analytical solution is not an absolute necessity. The advantages of an analytical solution are that it allows one to obtain an expression for the characteristic time of the heating process and that it reveals the major physical contributions leading to the predicted behavior. To solve Eq. (4) analytically, one must first linearize Eq. (2) with respect to temperature; the linearized result is then substituted into Eq. (4), and the resulting expression is integrated. [Clearly Eqs. (2) and (4) are also functions of the radius; however, as shown earlier,[4] for small values of the product $(I_0\alpha r_s^2)$, the effect of small variations in r_s on the steady state temperature is negligible.] Analogous to the development of Armstrong,[4] an expansion of Eq. (2) in a second-order Taylor series of the dimensionless temperature X [where $X = (T - T_\infty)/T_\infty$] yields for the mass flux

$$J = \frac{D_a}{r_s}(\epsilon X + \psi X^2), \tag{15}$$

where

$$\epsilon = \left(\frac{Y_\infty}{1 - Y_\infty}\right)\left(\frac{-A + B\delta + C}{T_\infty}\right),$$

$$\psi = \epsilon\left[\frac{(-A + B\delta + C)}{2(1 - Y_\infty)T_\infty} - 1 + \frac{B\beta T_\infty}{2(-A + B\delta + C)}\right].$$

Equation (15) is identical in form to Eq. (9) of Armstrong,[4] except that in the latter equation the constants A, B, δ, and β do not appear, and the Y_∞ term does not include the effect of the water activity on the vapor pressure. Additionally, the droplet density and heat capacity in Eq. (15) are those of a solution, whereas the corresponding properties in Ref. 4 apply to a pure water droplet. In the limit of zero molality and negligible Kelvin effect, the water activity coefficient approaches unity, and Eq. (15) reduces to that given by Armstrong.

When the radius does not change appreciably during the heating period, Eq. (15) can be substituted into Eq. (4) (after nondimensionalizing the temperature). The resulting expression is then integrated to yield the droplet temperature as a function of time:[4]

$$X(t) = \begin{cases} \dfrac{2l_0\tau_h[1 - \exp(-t/\tau_h)]}{1 + l_1\tau_h + (1 - l_1\tau_h)[\exp(-t/\tau_h)]} & \text{if } t \le t_p, \\ \dfrac{l_1 X(t_p)\exp(-l_1 t)}{l_1 + l_2 X(t_p)[1 - \exp(-l_1 t)]} & \text{if } t > t_p \end{cases} \tag{16}$$

where t_p is the heating period, $X(t_p)$ is the dimensionless temperature at the end of the heating period, and τ_h is the characteristic time for the heating process. The constants in Eq. (16) are given by

$$l_0 = \frac{I_0\alpha}{\rho_d C_d T_\infty}$$

$$l_1 = \frac{3}{\rho_d C_d r_s^2}\left(\frac{D_a L}{T_\infty}\epsilon + k_a\right)$$

$$l_2 = \frac{3}{\rho_d C_d r_s^2}\left(\frac{D_a L}{T_\infty}\psi - \frac{C_a D_a}{2}\epsilon\right),$$

$$\tau_h = (l_1^2 + 4l_0 l_2)^{-1/2}.$$

III. Thermodynamic Data

In the evaluation of Eq. (16) we used activity coefficient data reported by Hamer and Wu[9] for NaCl at 298 K. The computation of the temperature dependence of the activity coefficient requires data on the partial molal enthalpy and heat capacity. This information [used in Eqs. (11) and (12)] was obtained by fitting tabulated data[10] to a power series in terms of molality. The following expressions were calculated for the relative apparent partial molal enthalpy and heat capacity (valid in the range of $0.1 < m < 6.0$):

Table I. Summary of the Values of Various Physical Constants used in the Calculation (at 298 K)

Symbol	Value	Units
T_∞	298.15	K
Y^0	2.0×10^{-2}	Dimensionless
L	584.0	cal g^{-1}
$I_0\,\alpha$	10^5, 10^8	W cm^{-3}
C_a	0.25	cal g^{-1} K^{-1}
D_a	3.0×10^{-4}	g cm^{-1} sec^{-1}
k_a	6.2×10^{-5}	cal cm^{-1} sec^{-1} K^{-1}
M_a	28.39	g $mole^{-1}$
M_2	58.45	g $mole^{-1}$
M_w	18.0	g $mole^{-1}$
ρ_w	0.997	g cm^{-3}
$\overline{C}_w^0$	1.0	cal g^{-1} K^{-1}
$\overline{C}_2^0$	−23.8	cal $mole^{-1}$ K^{-1}
σ	72.0	dyn cm^{-1}

[a] Subscripts w and 2 refer to the solvent (water) and solute, respectively.

$$\Phi_L = \Phi_H - \Phi_H^0 = 458.95m^{1/2} - 688.09m + 241.47m^{3/2} - 39.339m^2 + 4.3245m^{5/2} - 0.0449m^3, \quad (17)$$

$$\Phi_{Cp} - \Phi_{Cp}^0 = 10.291m^{1/2} - 3.6538m + 13.121m^{3/2} - 10.638m^2 + 3.5304m^{5/2} - 0.4282m^3, \quad (18)$$

where Φ_H and Φ_H^0 are the apparent partial molal enthalpy at molality m and at infinite dilution, respectively. [The terms in Eq. (18) have analogous meaning.] The units of Eqs. (17) and (18) are (cal $mole^{-1}$) and (cal $mole^{-1}$ K^{-1}), respectively.

The relative partial molal enthalpy and heat capacity are then calculated from[8]

$$\overline{H}_i - \overline{H}_i^0 = \Phi_L - m\frac{\partial \Phi_L}{\partial m}. \quad (19)$$

A similar expression yields the value of the relative partial molal heat capacity. The heat capacity of the solution is given by[8]

$$C_p = n_w\overline{C}_w^0 + n_2\Phi_{C_p}, \quad (20)$$

where n_w and n_2 refer to the number of moles of solvent (water) and the solute, respectively, and $\overline{C}_w^0$ is the molar heat capacity of pure water. Results from Eq. (20) agree well with the heat capacity data reported by Bromley *et al.*[11]

The density of a salt solution is given by[8]

$$\rho_d = \rho_d^0 + \frac{c}{1000}(M_2 - \Phi_V\rho_d^0), \quad (21)$$

where c is the solute concentration (in moles $liter^{-1}$), Φ_V is the solution apparent molal volume, and ρ_d^0 is the density of pure solvent. Data for Eq. (21) were taken from Ref. 8.

IV. Short-Time Heating of an NaCl Droplet

In this section we calculate the droplet temperature rise resulting from short-time laser heating of an aqueous NaCl droplet. The parameters used in the calculations are given in Table I. During short-time heating the evaporation rate is assumed to be slow enough that the drop's radius and concentration do not change significantly. To compare the drop temperature rise computed here with that given in the literature, we consider conditions similar to those used by other authors.[3,4]

In general, the water content of an aerosol particle depends on both the surrounding relative humidity and the solutes it contains. In the limit of low water vapor pressure (at temperature much lower than the boiling point), the water activity in the drop is approximately equal to the relative humidity (RH). Thus in the case of high RH (e.g., in clouds), the effect of solutes is expected to be minimal. However, at lower RH, or when the heating causes a significant increase in solute concentration, one expects the solute to have an increasing effect on the vaporization rate and temperature rise in the drop. Equation (16) was evaluated for the case of a water drop containing various molalities of sodium chloride. In all cases considered, the salt concentration was low enough that the drop was below the saturation point. (For NaCl the saturation point is reported[9] to be $m \approx 6.1$ at 298 K.)

The temperature rise as a function of the dimensionless heating time predicted by Eq. (16) is shown in Figs. 1 and 2. The main difference between Figs. 1 and 2 is in the magnitude of the heating $I_0\alpha$. Based on

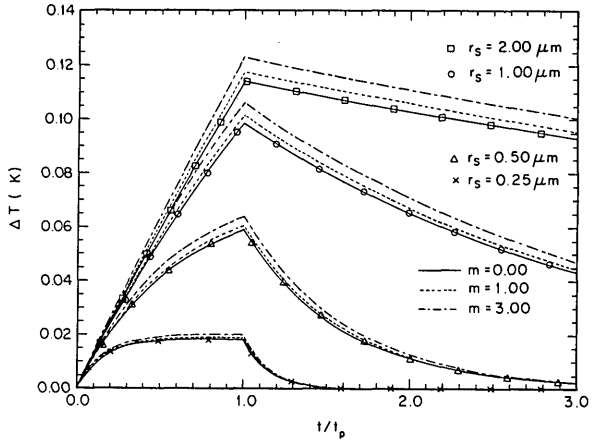

Fig. 1. Temperature rise in a droplet vs dimensionless time at t_p = 5 μsec; r_s = 0.25, 0.5, 1.0, 2.0 μm, and $I_0\alpha = 10^5$ W cm^{-3}.

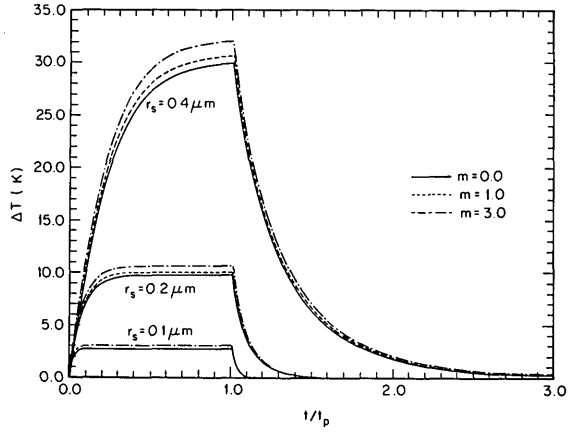

Fig. 2. Temperature rise in a droplet vs dimensionless time at t_p = 5 μsec; r_s = 0.10, 0.20, 0.40 μm, and $I_0\alpha = 10^8$ W cm^{-3}.

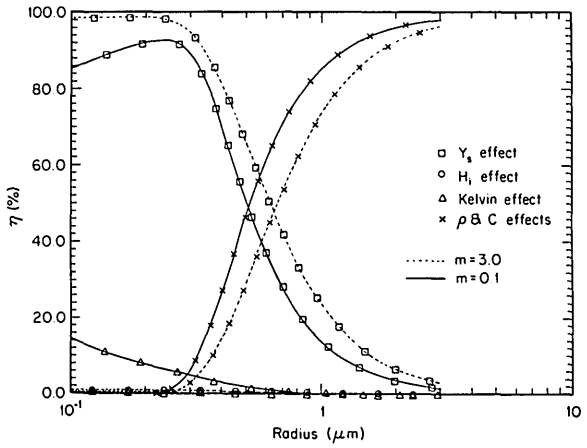

Fig. 3. Contribution of various parameters to the difference between the maximum temperature rise in a solution and that in a pure drop.

index of refraction data in Querry *et al.*,[12] the magnitude of α for an NaCl solution (irradiated by a laser having a wavelength of 9.09 μm) ranges from $\alpha = 595$ cm^{-1} for 1-M solution to $\alpha = 650$ cm^{-1} for 5-M solution (where M is the molar concentration). Thus I_0 was chosen to make $I_0\alpha = 10^8$ and $I_0\alpha = 10^5$ to simulate the heating caused by high and moderate beam intensities.

As seen from Figs. 1 and 2, the main effect of the solute is to increase the drop temperature rise above that which a pure droplet experiences. In all cases shown in Figs. 1 and 2 the maximum difference between the temperature rise of a solution and that in a pure drop is ~10%, a difference that increases with increasing salt concentration. As will be shown shortly, this deviation can be explained in terms of the differences among the densities, the heat capacities, and the vapor pressures of a solution and pure water droplet.

The deviations between the temperature rise in a solution droplet and that in a pure drop, shown in Figs. 1 and 2, are controlled by different parameters depending on the radius and concentration of the drop. To examine the effects of the vapor pressure Y_s, the partial molal quantities ($\overline{C}_i$ and $\overline{H}_i$), the solution density and heat capacity (ρ_d and C_d), and the Kelvin correction term, we define the quantity η as

$$\eta = \frac{T^* - T^0}{T^s - T^0} \times 100\%, \tag{22}$$

where T^0 and T^s are the maximum temperatures achieved in a pure water drop and in a solution, respectively, while T^* is the maximum temperature calculated by including only one of the parameters above in the equation for the temperature rise in a pure droplet. The parameters ρ_d and C_d were lumped together because they appear together in Eq. (4).

The values of η at various radii and molalities are shown in Fig. 3. It is evident that for large drops the difference between the density and heat capacity of a solution droplet and those of a pure droplet is responsible for the extra temperature rise of the solution. This effect occurs because the second term on the right-hand side of Eq. (4) is proportional to $1/r_s^2$, so as r_s increases the second term becomes less significant relative to the first term. In a NaCl solution the product of the density and heat capacity is smaller than the corresponding product in a pure drop; thus when the first term in Eq. (4) dominates (i.e., at large radii), the larger temperature rise in a solution is expected.

It is also apparent that the contribution of the solute partial molal enthalpy to the drop temperature rise is at most 1.0%. The effect of the partial molal heat capacity was <0.1%; therefore, it was omitted from Fig. 3. These results show that neglecting the partial molal terms in Eq. (14) does not lead to a serious error in the calculated temperature rise of the drop.

At the small radii in Fig. 3 the solution vapor pressure is responsible for the increased temperature rise. This pattern occurs because the interaction of solute molecules with the solvent lowers the vapor pressure of the solution. Since the initial vapor pressure over the drop is lower, the change in the vapor pressure during heating is lower. Because the mass flux from the drop is proportional to the change in the vapor pressure (to a first-order approximation), a solution droplet will evaporate less than a pure droplet for the same energy input. As a result of the smaller evaporation, the efficiency of evaporative cooling in a solution is lowered. The heat not dissipated by evaporation must then be removed by conduction; thus the drop's temperature must increase to raise the conduction driving force.

At very small radii (i.e., $r_s \ll 0.1$ μm) the Kelvin effect is expected to control the temperature rise in the drop. However, at these small radii the mean free path of the air molecules becomes comparable with the drop's radius; thus the solution presented here does not apply in that regime.

It should be pointed out that even in the case of a pure droplet the results presented here are slightly different from those reported by Armstrong,[4] because some of the parameters (mainly L and Y^0) were chosen differently. We used data on the heat of vaporization at the ambient temperature rather than at 373 K. We also used a different value of Y^0 because at the value used earlier[4] (Y^0 was 0.0138 at $T_\infty = 296$ K), the relative humidity was ~78%. However, for a pure water droplet to exist in equilibrium (at 298 K), the relative humidity must be 100% at which point $Y^0 \approx 0.020$.

Clearly, as the energy input ($I_0\alpha$) increases for a given drop size, the effects of the large temperature rise in the drop become increasingly important. To evaluate the validity of the analytical solution, we solved the full simultaneous heat and mass transfer equations numerically. A comparison of the analytical and numerical solutions for a 0.8-μm drop is shown in Fig. 4. It is evident from Fig. 4 that the discrepancy between the numerical and analytical solutions increases as the radiation intensity is increased. The top curve in Fig. 4 reveals that large deviations between the analytical and numerical solutions occur when $I_0\alpha r_s^2 = 0.64$ W cm^{-1}. At $I_0\alpha = 10^7$ the deviations occur mainly during the cooling period (at $t_p > 1.0$). It was pointed out by

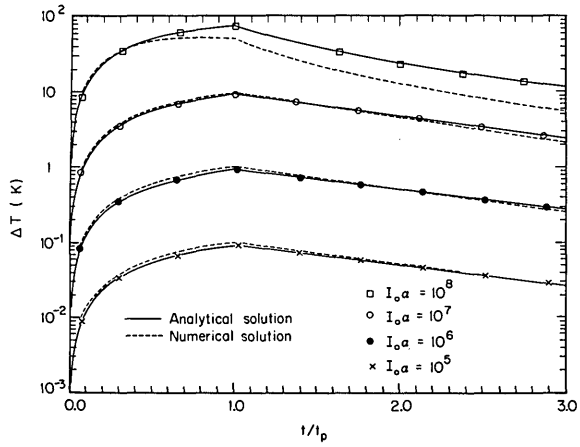

Fig. 4. Discrepancy between the analytical and numerical solutions for the short-time heating of a droplet of $m = 3.0$ and $r = 0.8$ μm.

Armstrong[4] that the analytical solution for a pure droplet is valid when the magnitude of the product $I_0 \alpha r_s^2$ is < 0.5. The results of Fig. 4 indicate that the deviations in a solution begin to occur at a smaller value of the product above.

The differences between the heating of a solution and a pure droplet become more pronounced as the heating period increases. In the next section the temperature and radius changes a solution droplet undergoes when heated for a long time period will be discussed.

V. Long-Time Heating of a NaCl Droplet

When a droplet is heated for an extended time period, its radius and molality change with time. As will be shown shortly, the drop pseudo-steady state temperature also changes with time. The initial increase in the drop temperature increases the surface vapor pressure of the drop, thereby inducing a net mass flux from the drop which lowers the drop's water activity. This process continues until a new equilibrium state, determined by Eq. (5), is reached. Hence, during long-time heating, the analytical solution developed earlier is no longer valid. To evaluate the temperature and radius of the drop, the following relation between the mass flux from the drop and the drop radius is used:

$$\frac{\partial r_s}{\partial t} = \frac{1}{\rho_d} J. \tag{23}$$

The temperature changes for various salt concentrations and heating rates were obtained by solving Eqs. (4) and (23) numerically, results of which are shown in Fig. 5. The quantity τ_d used in the nondimensionalization of the temperature corresponds to the time constant for vaporization of a pure water droplet; it is given by[4]

$$\tau_d = \frac{3\rho_d L(k_a + \Gamma)}{I_0 \alpha \Gamma}, \tag{24}$$

where

$$\Gamma = \frac{L^2 D_a M_w Y^0}{R(1 - Y^0) T_\infty^2}.$$

The parameter τ_d was chosen to scale the heating time to facilitate the comparison of the long-time heating of a solution droplet with that of a pure droplet.

As seen from Fig. 5, the temperature rise in a solution is quite different from the constant steady state temperature predicted by the analytical solution. This behavior results from the combination of two opposing effects. The first effect on the temperature rise is due to the decrease in the drop radius as a result of evaporation. Equation (16) shows that the temperature rise is proportional to τ_h; however, τ_h is proportional to the drop radius. Therefore, as the drop radius decreases due to evaporation the magnitude of the temperature rise the drop undergoes is expected to decrease as well. The decrease in the temperature during the heating period is also in agreement with results of Caledonia and Teare.[3]

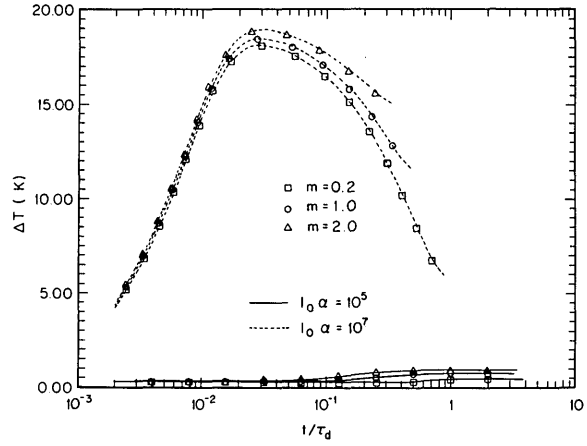

Fig. 5. Temperature rise vs dimensionless heating time for long-time heating of a droplet of initial radius $r_0 = 1.0$ μm, $\tau_d = 0.9435$ sec (at $I_0\alpha = 10^5$ W cm^{-3}), and $\tau_d = 0.009435$ sec (at $I_0\alpha = 10^7$ W cm^{-3}).

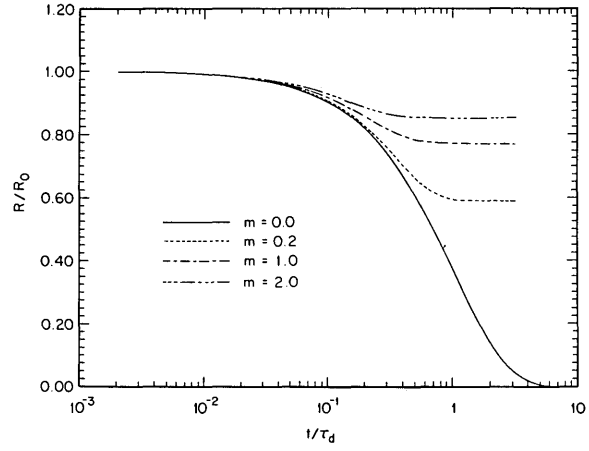

Fig. 6. Dimensionless radius vs dimensionless heating time for $r_0 = 1.0$ μm, and $\tau_d = 0.9435$ sec (at $I_0\alpha = 10^5$ W cm^{-3}).

The second effect on the drop temperature results from the decrease in the vaporization rate from the drop as it approaches a new equilibrium state. Since at equilibrium the net evaporation from the drop is zero, all the heat absorbed by the drop must be dissipated by conduction. The temperature of the drop must, therefore, increase to allow the larger conduction of heat away from the drop.

The two effects above oppose each other, thereby giving rise to the maximum observed in Fig. 5. The vaporization rate effect dominates when the changes in the radius are small and during the initial stage of the heating period. The effect of the decrease in radius begins to dominate only after sufficiently long heating times. The radius effect is less significant for the more concentrated drops simply because these drops undergo a smaller change in radius.

The variation of the drop radius with heating time, shown in Fig. 6, describes the approach of the droplet to its new equilibrium state. Also included in Fig. 6 is the radius change in a pure water droplet calculated from the analytical solution of Armstrong.[4] The radius of the pure droplet decreases continuously, and the process is eventually governed by the Kelvin effect.

As evident from Fig. 6 the dimensionless pure droplet evaporation time constant τ_d is larger than the corresponding time constant in a solution droplet. Additionally, for a given heating rate and drop size, the time required for the solution droplet to reach a new equilibrium size decreases as its salt concentration increases. This occurs because in the more concentrated drops less water needs to evaporate to lower the water activity to the point where a new equilibrium state is established. The smaller fractional change of radius in the more concentrated drops is also clearly demonstrated in Fig. 6.

VI. Conclusions

The laser-induced heating of both a pure water droplet and one containing various concentrations of NaCl has been determined both for short and long heating periods. For the case of short heating times, in which the drop radius does not change appreciably, an analytical solution for the drop temperature rise has been developed. This solution is an extension to Armstrong's[4] analytical solution to the temperature rise in a pure water droplet.

The full governing equations to the heating process were also solved numerically for the case of long heating periods. It was shown that the temperature and radial changes in the drop are strongly influenced by the incident beam intensity and the salt concentration in the drop.

The calculations here were done in terms of the parameter $I_0\alpha$. In a more general solution, the explicit concentration dependence of the bulk absorption coefficient α would be included.

References

1. H. C. van de Hulst, *Light Scattering by Small Particles* (Dover, New York, 1981).
2. A. Ashkin and J. M. Dziedzic, "Observations of Optical Resonances of Dielectric Spheres by Light Scattering," Appl. Opt. **20**, 1803 (1981).
3. G. E. Caledonia, and J. D. Teare, J. Heat Transfer **99**, 281 (1977).
4. R. L. Armstrong, "Aerosol Heating and Vaporization by Pulsed Light Beams," Appl. Opt. **23**, 148 (1984).
5. R. B. Bird, W. E. Stewart, and E. N. Lightfoot, *Transport Phenomena* (Wiley, New York, 1980).
6. F. A. Williams, "On Vaporization of Mist by Radiation," Int. J. Heat Mass Transfer **8**, 575 (1965).
7. A. W. Stelson and J. H. Seinfeld, "Relative Humidity and Temperature Dependence of the Ammonium Nitrate Dissociation Constant," Atmos. Environ. **16**, 983 (1982).
8. S. H. Harned and B. B. Owne, *The Physical Chemistry of Electrolytic Solutions* (Reinhold, New York, 1958).
9. W. J. Hamer and Y. C. Wu, "Osmotic Coefficients and Mean Activity Coefficients of Uni-Univalent Electrolytes in Water at 25°C," J. Phys. Chem. Ref. Data **1**, 1047 (1972).
10. H. F. Gibbard, G. Scatchard, R. A. Rousseau, and J. L. Creek, "Liquid-Vapor Equilibrium of Aqueous Sodium Chloride from 298 to 373 K and from 1 to 6 mole kg^{-1} and Related Properties," J. Chem. Eng. Data **19**, 281 (1974).
11. L. A. Bromley, A. E. Diamond, E. Salami, and D. G. Wilkins, "Heat Capacities and Enthalpies of Sea Salt Solutions to 200°C," J. Chem. Eng. Data **15**, 246 (1970).
12. M. R. Querry, R. C. Waring, W. A. Holand, G. M. Hale, and W. Nijm, "Optical Constants in IR for Aqueous NaCl," J. Opt. Soc. Am. **62**, 849 (1972).

This work was supported by U.S. Environmental Protection Agency grant R-810857. The authors wish to thank Stephen Arnold and Robert L. Armstrong for helpful input.